Y02

Proceedings of the 5th International Conference on Inverse Problems in Engineering: Theory and Practice, Cambridge, UK, 11-15th July 2005

A HYBRID DIFFUSION MODEL FOR 2D DENSE MOTION ESTIMATION

L. X. YANG, H. SAHLI and D. N. HAO
ETRO/IRIS, Vrije Universiteit Brussel, Pleinlaan 2, B-1050 Brussel - Belgium
e-mail: lxyang,hsahli,hao@etro.vub.ac.be

Abstract - 2D motion field is the velocity field which presents the apparent motion from one image to another in an image sequence. In this paper, with the objective of accurate estimation of 2D dense motion field, a hybrid diffusion model is proposed. The present approach differs from those in the literature in that the diffusion model and its associated objective functional are driven by both the flow field and image, through the nonlinear isotropic diffusion term and the linear anisotropic diffusion term, respectively. The diffusion function in the model is required to be non increasing, non negative, differentiable and bounded. Furthermore, using Schauder's fixed point theorem, we prove the existence, stability and uniqueness of the solution to the proposed hybrid diffusion model. The semi-implicit scheme is proposed to implement the hybrid diffusion model. We demonstrate its efficiency and accuracy by experiments on synthetic and real image sequences.

1. INTRODUCTION

Efficient and reliable 2D dense motion (optical flow) estimation plays a very important role in image processing and computer vision with various applications, such as dense depth estimation, motion analysis, etc. It can be formulated in terms of a variational problem which minimizes a specific energy functional. Recently variational techniques and associated PDE approaches have been widely applied for 2D motion estimation. They are efficient to regularize motion field while preserving important data discontinuities [17].

Apart from the standard Tikhonov quadratic regularization of Horn and Schunck's [10], Deriche *et al.* [7] investigated nonquadratic smoothness constraints. They used monotone flux functions for which one can guarantee well-posedness of the process. Proesmans *et al.* [16] developed the coupled geometry-driven diffusion equations to estimate optical flow. Their model is complicated, and composed of a system of six coupled nonlinear reaction diffusion equations. Weickert [19] improved the smoothness constraint of [7] by setting up a stronger coupling system of two nonlinear reaction diffusion equations with a common diffusivity for both components of optical flow ensuring that the discontinuities appear at the same locations. Alvarez *et al.* [2] incorporated the orientation smoothness term from [14] to form an anisotropic diffusion model, taking into account the orientation information from image sequence. Recently Brox *et al.* [4] introduced an extra data term from gradient constancy assumption, they obtained significantly improved estimation results.

In the literature, the diffusion process for optical flow estimation, is controlled by either the image gradient information (image driven), or the optical flow field information (flow driven). For example, nonlinear flow-driven isotropic diffusion models, only preserve the discontinuities in the magnitude of the optical flow [19]; while image-driven anisotropic diffusion models only consider the discontinuities in the gradient orientation [2]. There are seldom diffusion models which could take into account both discontinuities. Weickert and Schnörr [20] proposed a unifying framework to include different diffusion models. They focus on convex regularizers which can guarantee a unique minimum. However, there are indeed wide applications of non-convex regularizers in practice for more precisely handling discontinuities, such as Geman and Reynolds's model for recovery of discontinuities in image restoration [8] and Keeling and Stollberger's model for more accurate segmentation [11], etc.

In this work, we propose a hybrid diffusion model in order to make full use of the available information at each location of image sequence, i.e. image and optical flow field. Starting from a general energy functional which is not necessarily convex, we use the variational principle to formulate its associated Euler-Lagrange equations and set up the hybrid diffusion model. A system of coupled reaction diffusion equations, including both nonlinear flow driven diffusion term and anisotropic image driven diffusion term is proposed. This formulation allows preserving the discontinuities in magnitude and orientation with an attempt for more accurate estimation of motion field.

Throughout the literature, there is not much theoretical support provided to analyze the diffusion model properties, especially for non-convex regularizers. One of the fundamental investigations was made by Weickert [18] for the theoretical analysis of nonlinear diffusion filtering, to establish existence,

uniqueness and regularity of its solution, based on the mathematical formulation from [5].

For optical flow estimation, Alvarez *et al.* [1] developed a theoretical framework to prove the existence and uniqueness of solution for a linear inhomogeneous diffusion model. Their proposed model is associated with quadratic energy functional. For their theoretical analysis, the Banach fixed point theorem has been used, which only applies to contraction mapping. The same framework and theorem have been used to analyze a linear anisotropic diffusion model of [3]. Hinterberger *et al.* [9] studied the existence and uniqueness of solution to quasi-convex functionals. Recently, Weickert and Schnörr [20] provided the theoretical proof of well-posedness in the sense of Hadamard for convex regularizers.

In this work, following the framework proposed in [5], we prove the existence, stability and uniqueness of the solution to the proposed hybrid diffusion model for optical flow estimation which consists of two coupled PDEs. The Schauder fixed point theorem is used, which applies to infinite-dimensional Banach space and any continuous mapping, more stronger than the Banach fixed point theorem. Since our analysis is not restricted to convex regularizers, this provides theoretical support for the diffusion models with non-convex regularizers and more flexibility for the selection of regularizers in applications.

Furthermore, to implement the proposed model, the semi-implicit scheme is formulated. It is a stable and efficient numerical scheme. Experimental results on both synthetic and real image sequences show its advantages, i.e. fast convergence and high accuracy.

The rest of the paper is organized as follows, section 2 presents the hybrid diffusion model based on variational principle. Section 3 investigates the theoretical analysis of the model, and proves the existence, stability and uniqueness of solution to the model. In section 4, a semi-implicit scheme is proposed for the numerical implementation of the model. Section 5 presents experimental evaluation performed on both synthetic and real image sequences. Finally, some conclusions are drawn in section 6.

2. HYBRID DIFFUSION MODEL - SYSTEM FORMULATION

As mentioned above, the optical flow estimation is an ill-posed inverse problem, for which a regularization term is usually required, such that the optical flow field should be piecewise smooth. Such a term could be (a) image driven, in order to suppress smoothing at or across image boundaries and preserve the orientation discontinuities, or (b) optical flow driven, to reduce smoothing across motion discontinuities. The resulting diffusion models are controlled by either the image gradient or the optical flow gradient.

In order to make full use of the available information at each location, we investigate a hybrid diffusion model which takes into account both image and optical flow field. The proposed general objective functional is defined as follows:

$$E(\mathbf{v}) = \int_\Omega \alpha C(\mathbf{v}) dxdy + \beta_{of} \int_\Omega \Phi(\|\nabla u\|, \|\nabla v\|) dxdy + \beta_I \int_\Omega tr((\nabla \mathbf{v})^T D(\nabla I)(\nabla \mathbf{v})) dxdy \tag{1}$$

where

$$C(\mathbf{v}) = (I_x u + I_y v + I_t)^2, \quad D(\nabla I) = \begin{pmatrix} d_{11} & d_{12} \\ d_{21} & d_{22} \end{pmatrix}, \quad \nabla \mathbf{v} = \begin{pmatrix} u_x & v_x \\ u_y & v_y \end{pmatrix} \tag{2}$$

I stands for the image, and $\mathbf{v}(u, v)$ is the optical flow field. The first term in eqn. (1) stands for the standard optical flow constraint [10]. The second and third terms are regularization terms based on the optical flow gradient and the image gradient, respectively. $\alpha, \beta_{of}, \beta_I \geq 0$, are constants to control the contributions of these terms. Φ is a potential function that is not necessarily convex. $D(\nabla I)$ is a positive definite matrix [14].

The above model can preserve the discontinuities of both orientation and magnitude based on the two diffusion terms (regularization terms). Along the same research direction, recently, a systematic framework that links the diffusion and optical flow paradigms was presented by Weickert and Schnörr [20], assuming that the objective function is convex. They proved the well-posedness of its solution in the sense of Hadamard. In the following analysis of our model, the regularizers are not necessarily convex. This would offer more choices of the regularizers to control the expected objective functional.

Based on the variational principle, we can deduce the associated Euler-Lagrange equations of the above objective functional, which is the necessary condition of the solution to minimization of eqn. (1)(see [21] for a proof). Further introducing the scale parameter, we can obtain the proposed diffusion model as:

$$\begin{aligned} u_\theta &= div[\beta_{of} \tfrac{\Phi'(\|\nabla u\|, \|\nabla v\|)}{|\nabla u|} \nabla u + 2\beta_I D(\nabla I) \nabla u] - 2\alpha(I_x u + I_y v + I_t) I_x \\ v_\theta &= div[\beta_{of} \tfrac{\Phi'(\|\nabla u\|, \|\nabla v\|)}{|\nabla v|} \nabla v + 2\beta_I D(\nabla I) \nabla v] - 2\alpha(I_x u + I_y v + I_t) I_y \end{aligned} \tag{3}$$

where Φ' is the derivative of function Φ.

In the case where Φ is in the form of $\Phi(\|\nabla u\|^2 + \|\nabla v\|^2)$, we obtain the following diffusion models:

$$\begin{aligned} u_\theta &= div[\beta_{of} \Phi'(\|\nabla u\|^2 + \|\nabla v\|^2) \nabla u + 2\beta_I D(\nabla I) \nabla u] - 2\alpha(I_x u + I_y v + I_t) I_x \\ v_\theta &= div[\beta_{of} \Phi'(\|\nabla u\|^2 + \|\nabla v\|^2) \nabla v + 2\beta_I D(\nabla I) \nabla v] - 2\alpha(I_x u + I_y v + I_t) I_y \end{aligned} \tag{4}$$

The two regularization parameters β_{of} and β_I are chosen to balance the contribution of the flow field information and image flow information, respectively. It is obvious that, when $\beta_I = 0$, the obtained nonlinear isotropic diffusion model is a special case of eqns (4). The same holds for the anisotropic diffusion model, when $\beta_{of} = 0$.

3. THEORETICAL ANALYSIS - EXISTENCE, STABILITY AND UNIQUENESS OF SOLUTION

In this section, we will analyze the solutions of the hybrid diffusion model given by eqns (4). In the past, the theoretical analysis of diffusion models in terms of existence and uniqueness of solution has been mainly made for image filtering with the fundamental analysis from [5] developed for the case of one diffusion equation. Inspired by their methodology, and based on the properties of a system of PDEs in [12], we analyze the solution to the system of the two coupled nonlinear reaction diffusion equations given by eqns (4). We use Schauder's fixed point theorem to prove that the solution of the hybrid diffusion model exists, it is unique, and the system is well-posed.

Before going further, we first discuss the issue of smoothing inside the diffusion term. Catté *et al.* [5] introduced the convolution with Gaussian kernel G_σ in the original Perona-Malik formulation [15], i.e., using $\|\nabla I_\sigma\| = \|\nabla G_\sigma * I\|$ to replace $\|\nabla I\|$ in the diffusion function in order to prove the existence and uniqueness of a solution. Following the same idea, we introduce the Gaussian convolution with each component of the optical flow in the diffusion term of the proposed hybrid model.

Let $\sigma > 0$, and $G_\sigma = \frac{1}{\sqrt{2\pi\sigma}} \exp(-\frac{\|\mathbf{x}\|^2}{4\sigma})$ be the Gaussian filter. We denote $\|\nabla G_\sigma * u\| = [\sum_{i=1}^{2} (\frac{\partial G_\sigma}{\partial x_i} * \tilde{u})^2]^{\frac{1}{2}}$, $\|\nabla G_\sigma * v\| = [\sum_{i=1}^{2} (\frac{\partial G_\sigma}{\partial x_i} * \tilde{v})^2]^{\frac{1}{2}}$, where $\tilde{u}$ is a linear and continuous extension of u to $\mathbb{R}^2$ and $\tilde{v}$ is a linear and continuous extension of v to $\mathbb{R}^2$. They depend on the boundary condition on $\partial\Omega$ imposed on u and v.

Assuming for simplicity that u and v are defined on $[0,1] \times [0,1]$, for Neumann boundary condition, we can set (it follows the mirror mapping)

$$\begin{aligned} &\tilde{u}(x,y) = u(-x,y), -1 \le x \le 0, 0 \le y \le 1, \quad \tilde{u}(x,-y) = u(x,-y), 0 \le x \le 1, -1 \le y \le 0, \cdots \\ &\tilde{v}(x,y) = v(-x,y), -1 \le x \le 0, 0 \le y \le 1, \quad \tilde{v}(x,-y) = v(x,-y), 0 \le x \le 1, -1 \le y \le 0, \cdots \end{aligned}$$

Let $\Phi'(\|\nabla G_\sigma \star u\|^2 + \|\nabla G_\sigma \star v\|^2)$. g is a non-increasing, non-negative, differentiable and bounded function which tends to zero at infinity.

Theorem. Denote $[0, a_1] \times [0, a_2]$ by Ω, $\max(|I_x|, |I_y|) \le A, \max(|I_t|) \le B$. Let T, β_I, β_{of}, and α be positive constants. Suppose that $u^0, v^0 \in L^2(\Omega), Q_T = \Omega \times (0,T]$.

Then there exist unique functions $u, v \in C^\infty([0,T]; L^2(\Omega)) \cap L^2(0,T; H^1(\Omega))$ verifying, in the distributional sense, the system

$$\begin{aligned} &u_\theta - div[\beta_{of}\Phi'(\|\nabla G_\sigma * u\|^2 + \|\nabla G_\sigma * v\|^2)\nabla u + 2\beta_I D(\nabla I)\nabla u] + 2\alpha(I_x u + I_y v + I_t)I_x = 0 \\ &v_\theta - div[\beta_{of}\Phi'(\|\nabla G_\sigma * u\|^2 + \|\nabla G_\sigma * v\|^2)\nabla v + 2\beta_I D(\nabla I)\nabla v] + 2\alpha(I_x u + I_y v + I_t)I_y = 0 \end{aligned} \tag{5}$$

$$\frac{\partial u}{\partial n} = 0, \frac{\partial v}{\partial n} = 0, \quad on \quad \partial\Omega \times]0,T] \qquad and \qquad u(0) = u^0, v(0) = v^0 \tag{6}$$

This unique solution is in $C^\infty(]0,T[\times\Omega)$ and depends continuously on the initial values u^0 and v^0.

Proof. For the simplicity of the proof, without losing generality, we can set $2\beta_I = \beta_{of} = 2\alpha = 1$.

(a) Existence of a solution.

Similar to the framework of [5], we introduce the space $W(0,T) = \{w \in L^2(0,T; H^1(\Omega)), \frac{dw}{d\theta} \in L^2(0,T; (H^1(\Omega))')\}$. It is a Hilbert space for the graph norm [6]. And let $f_1 = I_x I_t, f_2 = I_y I_t$.

First of all, as deduced in [21], we can prove that there is a constant C_2, depending only on T and A such that

$$\|u\|^2_{L^\infty(0,T;L^2(\Omega))} + \|v\|^2_{L^\infty(0,T;L^2(\Omega))} \le C_2(\|u^0\|^2_{L^2(\Omega)} + \|v^0\|^2_{L^2(\Omega)} + A^2B^2T|\Omega|) \tag{7}$$

where $|\Omega|$ is the measure of Ω.

Let $w_1, w_2 \in W(0,T) \cap L^\infty(0,T; L^2(\Omega))$. Consider the problem (E_w) of a system of two coupled PDEs

$$\begin{aligned} U_\theta(w) \quad &-div[\Phi'(\|\nabla G_\sigma \star w_1\|^2 + \|\nabla G_\sigma \star w_2\|^2)\nabla U(w) + D(\nabla I)\nabla U(w)] \\ &+(I_x U(w) + I_y V(w) + I_t)I_x = 0 \\ V_\theta(w) \quad &-div[\Phi'(\|\nabla G_\sigma \star w_1\|^2 + \|\nabla G_\sigma \star w_2\|^2)\nabla V(w) + D(\nabla I)\nabla V(w)] \\ &+(I_x U(w) + I_y V(w) + I_t)I_y = 0 \end{aligned} \tag{8}$$

$$\frac{\partial U}{\partial n} = 0, \frac{\partial V}{\partial n} = 0, \quad on \quad \partial\Omega \times]0,T], \qquad and \quad U(\cdot,0) = u^0, V(\cdot,0) = v^0. \tag{9}$$

The solution (U, V) of the problem (E_w) is understood in the sense that they belong to $W(0,T) \cap L^\infty(0,T; L^2(\Omega))$ and satisfy the system (similar to [5] except that here we have a system of two coupled

PDEs)

$$\begin{array}{c} < U_\theta(w), \gamma_1 > + \int_\Omega \Phi'(\|\nabla G_\sigma * w_1\|^2 + \|\nabla G_\sigma * w_2\|^2)\nabla U(w)\nabla\gamma_1 dxdy \\ + \int_\Omega D\nabla U(w)\cdot\nabla\gamma_1 dxdy + \int_\Omega (I_x^2 U(w) + I_x I_y V(w))\gamma_1 dxdy + < f_1, \gamma_1 >= 0, \\ < V_\theta(w), \gamma_2 > + \int_\Omega \Phi'(\|\nabla G_\sigma * w_1\|^2 + \|\nabla G_\sigma * w_2\|^2)\nabla V(w)\nabla\gamma_2 dxdy \\ + \int_\Omega D\nabla V(w)\cdot\nabla\gamma_2 dxdy + \int_\Omega (I_y^2 V(w) + I_x I_y U(w))\gamma_2 dxdy + < f_2, \gamma_2 >= 0, \\ \forall\gamma_1 \in H^1(\Omega), \forall\gamma_2 \in H^1(\Omega), \text{a.e. in } [0,T]. \end{array}$$

where $< \cdot, \cdot >$ is the inner product in $L_2(\Omega)$.

Since $w_1, w_2 \in L^\infty(0,T,L^2(\Omega))$; Φ', G are C^∞, and $\|\nabla G_\sigma * w_1\|^2 + \|\nabla G_\sigma * w_2\|^2$ is lower bounded, we can deduce that $\Phi'(\|\nabla G_\sigma * \cdot\|^2 + \|\nabla G_\sigma * \cdot\|^2) \in L^\infty(0,T,C^\infty(\Omega))$.

Thus, since Φ' is non-increasing, there exists a constant ϱ such that $\Phi'(\|\nabla G_\sigma * w_1\|^2 + \|\nabla G_\sigma * w_2\|^2) \geq \varrho$, where ϱ depends only on $\Phi', G_\sigma, \|u^0\|_{L^2(\Omega)}, \|v^0\|_{L^2(\Omega)}, A, B$.

We define

$$\begin{array}{l} H^1(\Omega) = \{\hat{u}(x,y) \mid \hat{u} \in L^2(\Omega), \frac{\partial\hat{u}}{\partial x}, \frac{\partial\hat{u}}{\partial y} \in L^2(\Omega)\} \\ H^{1,0}(Q_T) = \{\hat{u}(x,y,\theta) \mid \hat{u} \in L^2(Q_T), \frac{\partial\hat{u}}{\partial x}, \frac{\partial\hat{u}}{\partial y} \in L^2(Q_T)\} \\ V_2^{1,0}(Q_T) = H^{1,0}(Q_T) \cap C([0,T], L_2(\Omega)) \end{array}$$

According to Theorem 1.1 in Chapter 7 [12](pp. 573) applied to the problem (E_w), we deduce that there is a unique solution (U,V) with $U, V \in V_2^{1,0}(Q_T)$ for the problem (E_w).

Now, following the same way to prove the Theorems 1 and 2 of Chapter 18 in [6] (pp. 509-517), we conclude that $\frac{dU}{d\theta}, \frac{dV}{d\theta} \in L^2(0,T;(H^1(\Omega))')$, and

$$\|U(w)\|_{L^2(0,T;H^1(\Omega))} + \|V(w)\|_{L^2(0,T;H^1(\Omega))} \leq C_1, \tag{10}$$

$$\|\frac{dU(w)}{d\theta}\|_{L^2(0,T;(H^1(\Omega))')} + \|\frac{dV(w)}{d\theta}\|_{L^2(0,T;(H^1(\Omega))')} \leq C_3, \tag{11}$$

$$\|U(w)\|_{L^\infty(0,T;L^2(\Omega))} + \|V(w)\|_{L^\infty(0,T;L^2(\Omega))} \leq C_2(\|u^0\|_{L^2(\Omega)} + \|v^0\|_{L^2(\Omega)} + A^2B^2T|\Omega|) \tag{12}$$

where C_1 and C_3 are constants that depend only on Φ', G and u^0, v^0.

These estimates lead us to introduce the subset W_0 of $W(0,T) \times W(0,T)$ defined by

$$\begin{array}{rc} W_0 = \{ & (w_1,w_2), w_1, w_2 \in W(0,T); \|w_1\|_{L^2(0,T;H^1(\Omega))} + \|w_2\|_{L^2(0,T;H^1(\Omega))} \leq C_1, \\ & \|\frac{dw_1}{d\theta}\|_{L^2(0,T;(H^1(\Omega))')} + \|\frac{dw_2}{d\theta}\|_{L^2(0,T;(H^1(\Omega))')} \leq C_3, \\ & \|w_1\|_{L^\infty(0,T;L^2(\Omega))} + \|w_2\|_{L^\infty(0,T;L^2(\Omega))} \leq C_2(\|u^0\|_{L^2(\Omega)} + \|v^0\|_{L^2(\Omega)} + A^2B^2T|\Omega|); \\ & w_1(0) = u^0, w_2(0) = v^0\} \end{array}$$

By eqns (10)-(12), $(U(w), V(w))$ is a mapping from W_0 into W_0. Moreover, W_0 is a nonempty, convex and weakly compact in $W(0,T) \times W(0,T)$.

Next, following the same idea of Catté et al. [5], we can prove that (U,V) is a weakly continuous mapping from W_0 into W_0. Then, applying Schauder's fixed point theorem, we can prove the existence of a solution to eqns (5) and (6).

(b) Stability of the solution.

To prove that the solution depends continuously on the initial data, we consider $(\bar{u}(0), \bar{v}(0))$, $(\hat{u}(0), \hat{v}(0))$ as two initial values of the problem in eqns (5), and $(\bar{u}, \bar{v})$, $(\hat{u}, \hat{v})$ the two corresponding solutions, for almost every $t \in [0,T]$,

$$\begin{array}{l} \frac{d\bar{u}}{d\theta} - div(\bar{\kappa}\nabla\bar{u}) - div(D(\nabla I)\nabla\bar{u}) + (I_x\bar{u} + I_y\bar{v} + I_t)I_x = 0 \\ \frac{d\bar{v}}{d\theta} - div(\bar{\kappa}\nabla\bar{v}) - div(D(\nabla I)\nabla\bar{v}) + (I_x\bar{u} + I_y\bar{v} + I_t)I_y = 0 \end{array} \tag{13}$$

$$\begin{array}{l} \frac{d\hat{u}}{d\theta} - div(\hat{\kappa}\nabla\hat{u}) - div(D(\nabla I)\nabla\hat{u}) + (I_x\hat{u} + I_y\hat{v} + I_t)I_x = 0 \\ \frac{d\hat{v}}{d\theta} - div(\hat{\kappa}\nabla\hat{v}) - div(D(\nabla I)\nabla\hat{v}) + (I_x\hat{u} + I_y\hat{v} + I_t)I_y = 0 \end{array} \tag{14}$$

where $\bar{\kappa} = \Phi'(\|\nabla G_\sigma * \bar{u}\|^2 + \|\nabla G_\sigma * \bar{v}\|^2), \hat{\kappa} = \Phi'(\|\nabla G_\sigma * \hat{u}\|^2 + \|\nabla G_\sigma * \hat{v}\|^2)$

Similar to [5] except that we work on a system of two PDEs that contain two diffusion terms, we subtract the first equation in eqns (14) from the first one in eqns (13), and the second equation in eqns (14) from the second one in eqns (13), respectively, followed by multiplying the first equation by $\bar{u} - \hat{u}$, and the second equation by $\bar{v} - \hat{v}$, and integrating w.r.t. x, respectively, we obtain:

$$\begin{array}{ll} \int_\Omega div((\bar{\kappa} - \hat{\kappa})\nabla\hat{u})(\bar{u} - \hat{u})dxdy & = \int_\Omega \frac{d}{d\theta}(\bar{u} - \hat{u})(\bar{u} - \hat{u})dxdy - \int_\Omega div(\bar{\kappa}(\nabla\bar{u} - \nabla\hat{u}))(\bar{u} - \hat{u})dxdy \\ & - \int_\Omega div(D(\nabla I)(\nabla\bar{u} - \nabla\hat{u}))(\bar{u} - \hat{u})dxdy \\ & + \int_\Omega I_x^2(\bar{u} - \hat{u})^2 dxdy + \int_\Omega I_x I_y(\bar{v} - \hat{v})(\bar{u} - \hat{u})dxdy \\ \int_\Omega div((\bar{\kappa} - \hat{\kappa})\nabla\hat{v})(\bar{v} - \hat{v})dxdy & = \int_\Omega \frac{d}{d\theta}(\bar{v} - \hat{v})(\bar{v} - \hat{v})dxdy - \int_\Omega div(\bar{\kappa}(\nabla\bar{v} - \nabla\hat{v}))(\bar{v} - \hat{v})dxdy \\ & - \int_\Omega div(D(\nabla I)(\nabla\bar{v} - \nabla\hat{v}))(\bar{v} - \hat{v})dxdy \\ & + \int_\Omega I_y^2(\bar{v} - \hat{v})^2 dxdy + \int_\Omega I_x I_y(\bar{v} - \hat{v})(\bar{u} - \hat{u})dxdy \end{array} \tag{15}$$

Furthermore, we deduce

$$\begin{array}{ll} -\int_\Omega(\bar\kappa-\hat\kappa)\nabla\hat u(\nabla\bar u-\nabla\hat u)dxdy & =\frac{1}{2}\frac{d}{d\theta}\|\bar u-\hat u\|^2_{L^2(\Omega)}+\int_\Omega\bar\kappa(\nabla\bar u-\nabla\hat u)^2dxdy \\ & +\int_\Omega div(D(\nabla I)(\nabla\bar u-\nabla\hat u)\cdot(\nabla\bar u-\nabla\hat u)dxdy \\ & +\int_\Omega I_x^2(\bar u-\hat u)^2dxdy+\int_\Omega I_xI_y(\bar v-\hat v)(\bar u-\hat u)dxdy \\ -\int_\Omega(\bar\kappa-\hat\kappa)\nabla\hat v(\nabla\bar v-\nabla\hat v)dxdy & =\frac{1}{2}\frac{d}{d\theta}\|\bar v-\hat v\|^2_{L^2(\Omega)}+\int_\Omega\bar\kappa(\nabla\bar v-\nabla\hat v)^2dxdy \\ & +\int_\Omega div(D(\nabla I)(\nabla\bar v-\nabla\hat v)\cdot(\nabla\bar v-\nabla\hat v)dxdy \\ & +\int_\Omega I_y^2(\bar v-\hat v)^2dxdy+\int_\Omega I_xI_y(\bar v-\hat v)(\bar u-\hat u)dxdy \end{array} \tag{16}$$

Since $\bar\kappa$ is bounded from below by $\varrho\geq 0$ and $D(\nabla I)(\nabla\bar u-\nabla\hat u)\cdot(\nabla\bar u-\nabla\hat u)\geq 0$, we have

$$\begin{array}{l} \frac{1}{2}\frac{d}{d\theta}\|\bar u-\hat u\|^2_{L^2(\Omega)}+\varrho\|\nabla\bar u-\nabla\hat u\|_{L^2(\Omega)}+\int_\Omega I_x^2(\bar u-\hat u)^2dxdy \\ +\int_\Omega I_xI_y(\bar v-\hat v)(\bar u-\hat u)dxdy\leq\|\bar\kappa-\hat\kappa\|_{L^\infty(\Omega)}\|\nabla\hat u\|_{L^2(\Omega)}\|\nabla\bar u-\nabla\hat u\|_{L^2(\Omega)} \\ \frac{1}{2}\frac{d}{d\theta}\|\bar v-\hat v\|^2_{L^2(\Omega)}+\varrho\|\nabla\bar v-\nabla\hat v\|_{L^2(\Omega)}+\int_\Omega I_y^2(\bar v-\hat v)^2dxdy \\ +\int_\Omega I_xI_y(\bar v-\hat v)(\bar u-\hat u)dxdy\leq\|\bar\kappa-\hat\kappa\|_{L^\infty(\Omega)}\|\nabla\hat v\|_{L^2(\Omega)}\|\nabla\bar v-\nabla\hat v\|_{L^2(\Omega)} \end{array} \tag{17}$$

Taking the sum of the two equations in eqns (17), we get

$$\begin{array}{l} \frac{1}{2}\frac{d}{d\theta}\|\bar u-\hat u\|^2_{L^2(\Omega)}+\frac{1}{2}\frac{d}{d\theta}\|\bar v-\hat v\|^2_{L^2(\Omega)}+\varrho\|\nabla\bar u-\nabla\hat u\|^2_{L^2(\Omega)} \\ +\varrho\|\nabla\bar v-\nabla\hat v\|^2_{L^2(\Omega)}+\int_\Omega(I_x(\bar u-\hat u)-I_y(\bar v-\hat v))^2dxdy\leq \\ \|\bar\kappa-\hat\kappa\|_{L^\infty(\Omega)}\|\nabla\hat u\|_{L^2(\Omega)}\|\nabla\bar u-\nabla\hat u\|_{L^2(\Omega)}+\|\bar\kappa-\hat\kappa\|_{L^\infty(\Omega)}\|\nabla\hat v\|_{L^2(\Omega)}\|\nabla\bar v-\nabla\hat v\|_{L^2(\Omega)} \end{array} \tag{18}$$

Since Φ' and G are C^∞, $\|\bar\kappa-\hat\kappa\|_{L^\infty(\Omega)}\leq C_k(\|\bar u-\hat u\|_{L^2(\Omega)}+\|\bar v-\hat v\|_{L^2(\Omega)})$ with C_k depending on Φ', G and u^0, v^0. Using the fact that if $K_1, K_2>0$, then $K_1K_2\leq\frac{1}{4\varrho}K_1^2+\varrho K_2^2$, we get

$$\begin{array}{l} \frac{1}{2}\frac{d}{d\theta}\|\bar u-\hat u\|^2_{L^2(\Omega)}+\frac{1}{2}\frac{d}{d\theta}\|\bar v-\hat v\|^2_{L^2(\Omega)} \\ +\varrho\|\nabla\bar u-\nabla\hat u\|^2_{L^2(\Omega)}+\varrho\|\nabla\bar v-\nabla\hat v\|^2_{L^2(\Omega)}+\|I_x(\bar u-\hat u)-I_y(\bar v-\hat v)\|^2_{L^2(\Omega)} \\ \leq\frac{1}{4\varrho}C_k^2(\|\bar u-\hat u\|_{L^2(\Omega)}+|\bar v-\hat v\|_{L^2(\Omega)})^2\|\nabla\hat u\|^2_{L^2(\Omega)}+\varrho\|\nabla\bar u-\nabla\hat u\|^2_{L^2(\Omega)} \\ +\frac{1}{4\varrho}C_k^2(\|\bar u-\hat u\|_{L^2(\Omega)}+|\bar v-\hat v\|_{L^2(\Omega)})^2\|\nabla\hat v\|^2_{L^2(\Omega)}+\varrho\|\nabla\bar v-\nabla\hat v\|^2_{L^2(\Omega)} \end{array} \tag{19}$$

and so,

$$\frac{d}{d\theta}(\|\bar u-\hat u\|^2_{L^2(\Omega)}+\|\bar v-\hat v\|^2_{L^2(\Omega)})\leq\frac{1}{2\varrho}C_k^2(\|\nabla\hat u\|^2_{L^2(\Omega)}+\|\nabla\hat v\|^2_{L^2(\Omega)})(\|\bar u-\hat u\|_{L^2(\Omega)}+\|\bar v-\hat v\|_{L^2(\Omega)})^2 \tag{20}$$

Since $\|\nabla\hat u\|^2_{L^2(\Omega)}$ and $\|\nabla\hat v\|^2_{L^2(\Omega)}$ are bounded ($\|\nabla\hat u\|^2_{L^2(\Omega)}, \|\nabla\hat v\|^2_{L^2(\Omega)}\leq\bar C$), from Eqn. (20) we have

$$\frac{d}{d\theta}(\|\bar u-\hat u\|^2_{L^2(\Omega)}+\|\bar v-\hat v\|^2_{L^2(\Omega)})\leq\frac{1}{\varrho}C_k^2\bar C(\|\bar u-\hat u\|^2_{L^2(\Omega)}+\|\bar v-\hat v\|^2_{L^2(\Omega)}) \tag{21}$$

Taking the integral w.r.t. θ from 0 to τ, we get

$$\begin{array}{ll} \|\bar u-\hat u\|^2_{L^2(\Omega)}+\|\bar v-\hat v\|^2_{L^2(\Omega)} & \leq\frac{1}{\varrho}C_k^2\bar C\int_0^\tau(\|\bar u-\hat u\|^2_{L^2(\Omega)}+\|\bar v-\hat v\|^2_{L^2(\Omega)})d\theta \\ & +\|\bar u(0)-\hat u(0)\|^2_{L^2(\Omega)}+\|\bar v(0)-\hat v(0)\|^2_{L^2(\Omega)} \end{array} \tag{22}$$

Using the Gronwall lemma, we get

$$\|\bar u-\hat u\|^2_{L^2(\Omega)}+\|\bar v-\hat v\|^2_{L^2(\Omega)}\leq C_4(\|\bar u(0)-\hat u(0)\|^2_{L^2(\Omega)}+\|\bar v(0)-\hat v(0)\|^2_{L^2(\Omega)}) \tag{23}$$

with $C_4=\exp(\frac{1}{\varrho}C_k^2\bar CT)$.

Let $\epsilon>0$ and $\delta=\frac{\epsilon}{C_4}$. For $(\|\bar u(0)-\hat u(0)\|^2_{L^2(\Omega)}+\|\bar v(0)-\hat v(0)\|^2_{L^2(\Omega)})<\delta$, we have

$$\|\bar u-\hat u\|^2_{L^2(\Omega)}+\|\bar v-\hat v\|^2_{L^2(\Omega)}\leq\epsilon \tag{24}$$

This proves the continuous dependence of the solution on the initial data.

(c) Uniqueness of the solution.

Let $(\bar u,\bar v),(\hat u,\hat v)$ be two solutions of the problem in eqns (5), with the same initial value, i.e., $\bar u(0)=\hat u(0), \bar v(0)=\hat v(0)$.

Following the proof of stability, we can get eqn. (21). Taking the integral w.r.t. θ from 0 to τ, and noting that the initial conditions, $\bar u(0)=\hat u(0)=u^0, \bar v(0)=\hat v(0)=v^0$, we deduce

$$\|\bar u-\hat u\|^2_{L^2(\Omega)}+\|\bar v-\hat v\|^2_{L^2(\Omega)}\leq\frac{1}{\varrho}C_k^2\bar C\int_0^\tau(\|\bar u-\hat u\|^2_{L^2(\Omega)}+\|\bar v-\hat v\|^2_{L^2(\Omega)})d\theta \tag{25}$$

Using the Gronwall lemma, we obtain $\|\bar{u}-\hat{u}\|^2_{L^2(\Omega)}+\|\bar{v}-\hat{v}\|^2_{L^2(\Omega)}\leq 0$.
This concludes the uniqueness of the solution. ■

4. NUMERICAL SCHEME

Considering both stability and accuracy, we propose a semi-implicit scheme for implementing the proposed hybrid diffusion model. We discretize both the flow-driven and image-drive diffusion terms in the explicit way, and the reaction term in partially implicit way. The formulation can be set up as

$$\begin{array}{ll}\frac{u^{k+1}-u^k}{\tau} & =\beta_{of}\sum_{l=1}^{2}(A_f)_l(u^k,v^k)u^{k+1}+2\beta_I\sum_{l=1}^{2}(A_I)_l u^{k+1}-2\alpha(I_x u^{k+1}+I_y v^k+I_t)I_x\\ \frac{v^{k+1}-v^k}{\tau} & =\beta_{of}\sum_{l=1}^{2}(A_f)_l(u^k,v^k)v^{k+1}+2\beta_I\sum_{l=1}^{2}(A_I)_l v^{k+1}-2\alpha(I_x u^k+I_y v^{k+1}+I_t)I_y\end{array} \tag{26}$$

where τ is the scale step, $(A_f)_1$ and $(A_f)_2$ are matrices from standard finite difference approximations to the nonlinear isotropic diffusion term:

$$\begin{array}{l}A_1\leftarrow\partial_x(gv_{1,x})=\begin{cases}\frac{g_{i,j}+g_{n,j}}{2h_1^2} & (n\in\aleph(i))\\ -\sum_{n\in\aleph(i)}\frac{g_{i,j}+g_{n,j}}{2h_1^2} & (j=i)\\ 0 & otherwise\end{cases}\\ A_2\leftarrow\partial_y(gv_{1,y})=\begin{cases}\frac{g_{i,j}+g_{i,n}}{2h_2^2} & (n\in\aleph(j))\\ -\sum_{n\in\aleph(j)}\frac{g_{i,j}+g_{i,n}}{2h_2^2} & (j=i)\\ 0 & otherwise\end{cases}\end{array} \tag{27}$$

where (i,j) refers to the pixel points, $1\leq i\leq M, 1\leq j\leq N$, $\aleph(i)$ is the set of neighbors of i. h_1 and h_2 denote the pixel size in x and y direction, respectively. $g^k_{i,j}$ is the approximation of $\Phi'(\|\nabla G_\sigma * u\|^2+\|\nabla G_\sigma * v\|^2)$ at step k on pixel (i,j). $(A_I)_1$ and $(A_I)_2$ are matrices from finite difference approximations to the anisotropic diffusion term.

To clearly describe the expression from the discretization of the two diffusion terms and analyze the system structure, eqns (26) can be further written as follows

$$\begin{array}{l}(u^{k+1})_{i,j}\{\frac{1}{\tau}+\beta_{of}[\frac{g^k_{i+1,j}+g^k_{i,j}}{2h_1^2}+\frac{g^k_{i-1,j}+g^k_{i,j}}{2h_1^2}+\frac{g^k_{i,j+1}+g^k_{i,j}}{2h_2^2}+\frac{g^k_{i,j-1}+g^k_{i,j}}{2h_2^2}]\\ +2\beta_I[\frac{(d_{11})_{i+1,j}+(d_{11})_{i,j}}{2h_1^2}+\frac{(d_{11})_{i-1,j}+(d_{11})_{i,j}}{2h_1^2}+\frac{(d_{22})_{i,j+1}+(d_{22})_{i,j}}{2h_2^2}+\frac{(d_{22})_{i,j-1}+(d_{22})_{i,j}}{2h_2^2}\\ +\frac{(d_{12})_{i+1,j+1}+(d_{12})_{i,j}}{2h_1h_2}+\frac{(d_{12})_{i-1,j-1}+(d_{12})_{i,j}}{2h_1h_2}-\frac{(d_{12})_{i+1,j-1}+(d_{12})_{i,j}}{2h_1h_2}-\frac{(d_{12})_{i-1,j+1}+(d_{12})_{i,j}}{2h_1h_2}]+2\alpha {I_x}^2(\mathbf{x}_{i,j})\}\\ +(u^{k+1})_{i,j+1}\{-\beta_{of}\frac{g^k_{i,j+1}+g^k_{i,j}}{2h_1^2}-2\beta_I\frac{(d_{22})_{i,j+1}+(d_{22})_{i,j}}{2h_2^2}\}+(u^{k+1})_{i-1,j+1}\{2\beta_I\frac{(d_{12})_{i-1,j+1}+(d_{12})_{i,j}}{2h_1h_2}\}\\ +(u^{k+1})_{i+1,j}\{-\beta_{of}\frac{g^k_{i+1,j}+g^k_{i,j}}{2h_1^2}-2\beta_I\frac{(d_{11})_{i+1,j}+(d_{11})_{i,j}}{2h_1^2}\}+(u^{k+1})_{i+1,j+1}\{-2\beta_I\frac{(d_{12})_{i+1,j+1}+(d_{12})_{i,j}}{2h_1h_2}\}\\ +(u^{k+1})_{i+1,j-1}\{2\beta_I\frac{(d_{12})_{i+1,j-1}+(d_{22})_{i,j}}{2h_1h_2}\}+(u^{k+1})_{i-1,j}\{-\beta_{of}\frac{g^k_{i-1,j}+g^k_{i,j}}{2h_1^2}-2\beta_I\frac{(d_{11})_{i-1,j}+(d_{11})_{i,j}}{2h_1^2}\}\\ +(u^{k+1})_{i,j-1}\{-\beta_{of}\frac{g^k_{i,j-1}+g^k_{i,j}}{2h_2^2}-2\beta_I\frac{(d_{22})_{i,j-1}+(d_{22})_{i,j}}{2h_2^2}\}+(u^{k+1})_{i-1,j-1}\{-2\beta_I\frac{(d_{12})_{i-1,j-1}+(d_{12})_{i,j}}{2h_1h_2}\}\\ =\frac{1}{\tau}(u^k)_{i,j}-2\alpha I_x(\mathbf{x}_{i,j})I_y(\mathbf{x}_{i,j})(v^k)_{i,j}-2\alpha I_x(\mathbf{x}_{i,j})I_t(\mathbf{x}_{i,j})\end{array} \tag{28}$$

$$\begin{array}{l}(v^{k+1})_{i,j}\{\frac{1}{\tau}+\beta_{of}[\frac{g^k_{i+1,j}+g^k_{i,j}}{2h_1^2}+\frac{g^k_{i-1,j}+g^k_{i,j}}{2h_1^2}+\frac{g^k_{i,j+1}+g^k_{i,j}}{2h_2^2}+\frac{g^k_{i,j-1}+g^k_{i,j}}{2h_2^2}]\\ +2\beta_I[\frac{(d_{11})_{i+1,j}+(d_{11})_{i,j}}{2h_1^2}+\frac{(d_{11})_{i-1,j}+(d_{11})_{i,j}}{2h_1^2}+\frac{(d_{22})_{i,j+1}+(d_{22})_{i,j}}{2h_2^2}+\frac{(d_{22})_{i,j-1}+(d_{22})_{i,j}}{2h_2^2}\\ +\frac{(d_{12})_{i+1,j+1}+(d_{12})_{i,j}}{2h_1h_2}+\frac{(d_{12})_{i-1,j-1}+(d_{12})_{i,j}}{2h_1h_2}-\frac{(d_{12})_{i+1,j-1}+(d_{12})_{i,j}}{2h_1h_2}-\frac{(d_{12})_{i-1,j+1}+(d_{12})_{i,j}}{2h_1h_2}]+2\alpha {I_x}^2(\mathbf{x}_{i,j})\}\\ +(v^{k+1})_{i,j+1}\{-\beta_{of}\frac{g^k_{i,j+1}+g^k_{i,j}}{2h_1^2}-2\beta_I\frac{(d_{22})_{i,j+1}+(d_{22})_{i,j}}{2h_2^2}\}+(v^{k+1})_{i-1,j+1}\{2\beta_I\frac{(d_{12})_{i-1,j+1}+(d_{12})_{i,j}}{2h_1h_2}\}\\ +(v^{k+1})_{i+1,j}\{-\beta_{of}\frac{g^k_{i+1,j}+g^k_{i,j}}{2h_1^2}-2\beta_I\frac{(d_{11})_{i+1,j}+(d_{11})_{i,j}}{2h_1^2}\}+(v^{k+1})_{i+1,j+1}\{-2\beta_I\frac{(d_{12})_{i+1,j+1}+(d_{12})_{i,j}}{2h_1h_2}\}\\ +(v^{k+1})_{i+1,j-1}\{2\beta_I\frac{(d_{12})_{i+1,j-1}+(d_{22})_{i,j}}{2h_1h_2}\}+(v^{k+1})_{i-1,j}\{-\beta_{of}\frac{g^k_{i-1,j}+g^k_{i,j}}{2h_1^2}-2\beta_I\frac{(d_{11})_{i-1,j}+(d_{11})_{i,j}}{2h_1^2}\}\\ +(v^{k+1})_{i,j-1}\{-\beta_{of}\frac{g^k_{i,j-1}+g^k_{i,j}}{2h_2^2}-2\beta_I\frac{(d_{22})_{i,j-1}+(d_{22})_{i,j}}{2h_2^2}\}+(v^{k+1})_{i-1,j-1}\{-2\beta_I\frac{(d_{12})_{i-1,j-1}+(d_{12})_{i,j}}{2h_1h_2}\}\\ =\frac{1}{\tau}(v^k)_{i,j}-2\alpha I_x(\mathbf{x}_{i,j})I_y(\mathbf{x}_{i,j})(u^k)_{i,j}-2\alpha I_y(\mathbf{x}_{i,j})I_t(\mathbf{x}_{i,j})\end{array} \tag{29}$$

The two system matrices from eqns (28) and (29) are diagonal dominant, which guarantees the stability of the semi-implicit scheme.

5. EXPERIMENTAL RESULTS

This section presents the performance of the hybrid diffusion model using the semi-implicit scheme. Both synthetic and real natural image sequences are used. For the synthetic sequences, we use ground truth data to evaluate precisely the performance in a quantitative way. As 2D correct motion fields are available,

one of the popular error measurements is the angular error between the correct velocity and estimated one:

$$\psi_e = \arccos\left(\frac{u_c u_e + v_c v_e + 1}{\sqrt{(u_c^2 + v_c^2 + 1)(u_e^2 + v_e^2 + 1)}}\right) \tag{30}$$

where (u_c, v_c) denotes the correct velocity, and (u_e, v_e) is the estimated one.

For the real natural image sequences, we use the reconstruction error to evaluate the results. The estimated optical flow is used to project the second image back to the first one, and calculate how the reconstructed image differ from the original one.

In our experiments, we use a 3D Gaussian filter to smooth the image sequences. The smoothing of the gradient of optical flow during the diffusion process is fulfilled by convolution with the Gaussian derivative operator.

Synthetic sequence: First, we use the Yosemite sequence, which is a complex and challenging test sequence. It has a wide range of velocities, occluding edges, severe aliasing in the lower part of the scene. Clouds move from left to right at the top, and there exists a divergent motion starting from the upper right corner of the scene.

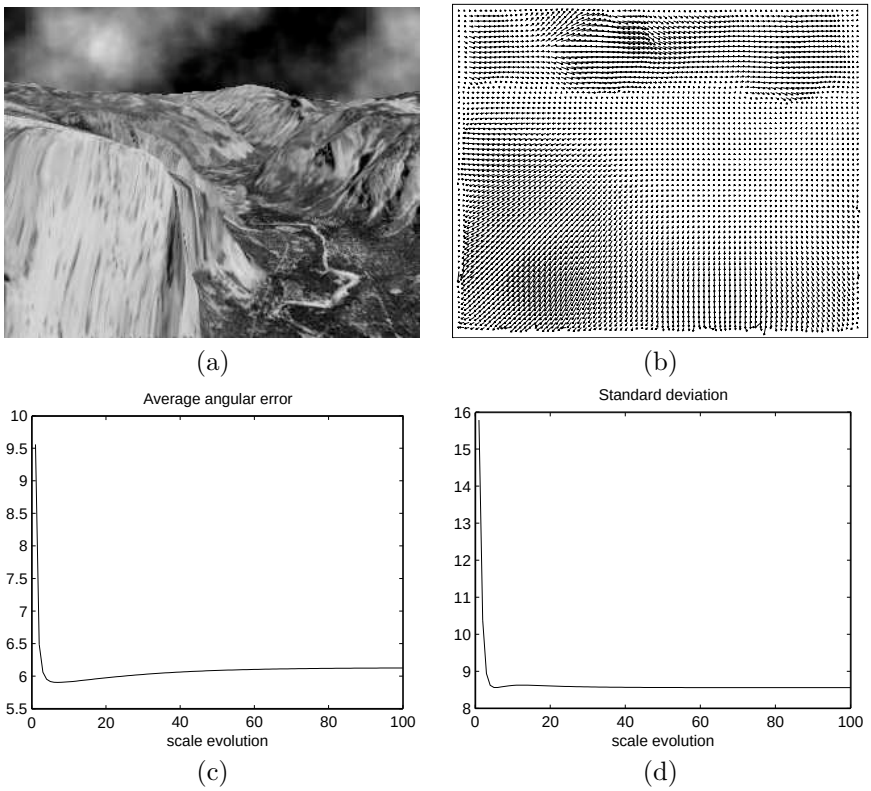

Figure 1. Performance on Yosemite sequence, with $\alpha = 0.001, \tau = 3.0, \lambda_{of} = 0.05, \lambda_I = 0.5, \beta_{of} = 1.0, \beta_I = 0.002$, (a) image #10, (b) optical flow needle map, (c) average angular error, (d) standard deviation.

The semi-implicit scheme is implemented for the hybrid diffusion model as described in eqns (28) and (29). Its performance is shown in Figure 1. With strong stability, the error drops dramatically at the first few steps and converges very fast with accurate estimation. Without restriction on scale step size, in this experiment τ is set to 3. The initial values are chosen from Horn's method.

To well demonstrate the properties of the proposed model, Figure 2 gives a comparison of different methods by illustrating the evolution of their error statistics for the first 200 scale steps (AOS(additive operator splitting), G-S (Gauss-Seidel) and Linear Multigrid are different implementation schemes for nonlinear isotropic diffusion model [21]). To evaluate the stability, we set the initial value of the optical flow to zero. The properties of the proposed hybrid diffusion model are obvious. As it can be seen, the hybrid diffusion model with the semi-implicit scheme has fast convergence and accurate estimation.

Table 1 summarizes the performance obtained using some existing methods, as well as the proposed one. One can notice that the proposed hybrid diffusion model with the semi-implicit scheme provides good estimation results, although it is not the best one. Considering the methods outperform the proposed one, Brox *et al.* [4] introduced gradient constancy constraint besides the standard brightness constancy

assumption; Mémin and Pérez [13] utilized the adaptive multigrid framework and robust estimators for data and regularization terms; Alvarez *et al.* [3] obtained the initial values by using a pyramid-based focusing algorithm, the scale step size was set to $\tau = 10$ with 50 iteration steps (the final scale is 500); while for the proposed hybrid diffusion model, the initial values could be simply set to zero, and the scale step size $\tau = 3$ with 40 iteration steps.

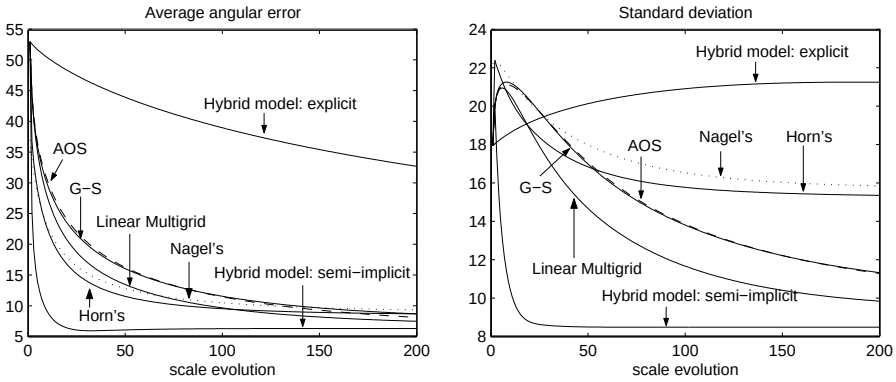

(a) (b)

Figure 2. Comparison of different schemes w.r.t., (a) average angular error, (b) standard deviation.

Technique	Average angular error	Standard deviation
Horn and Schunck (original)	31.69	31.18
Horn and Schunck (modified)	9.78	16.19
Nagel	10.22	16.51
Anandan (unthresholded)	13.36	15.64
Uras *et al.* (unthresholded)	8.94	15.61
Singh (step 1)	10.03	13.13
Alvarez[3]	5.53	7.40
Mémin and Pérez[13]	4.69	6.89
Brox *et al.* [4]	1.94	6.02
nonlinear isotropic diffusion (AOS scheme)	6.12	9.99
nonlinear isotropic diffusion (G-S solver)	6.13	10.03
nonlinear isotropic diffusion (linear MG solver)	6.09	9.09
Hybrid diffusion model (explicit scheme)	6.84	9.85
Hybrid diffusion model (semi-implicit scheme)	5.91	8.56

Table 1. Comparison between different methods for the Yosemite sequence

Real image sequence: Natural image sequences are used as well to evaluate the proposed diffusion model. Figure 3 presents the performance on Rubic sequence (Figure 3(a)), which consists of a cube rotating counter-clockwise on a turning table in the scene. Due to the stability of the semi-implicit scheme, the scale step size has been set to $\tau = 4$. As expected, the semi-implicit scheme provides good estimations with detailed discontinuities in limited iteration steps. Its reconstruction RMS decreases dramatically and converges after 15 steps, while the explicit scheme takes 200 steps before convergence.

We can observe that precise motion field without over-smoothing, as well as detailed discontinuities are obtained using the hybrid diffusion model with the semi-implicit scheme.

Figure 3(d) illustrates the comparison of the different methods we present here in terms of reconstruction RMS for first 50 scale steps. These results further validate the properties we discussed above.

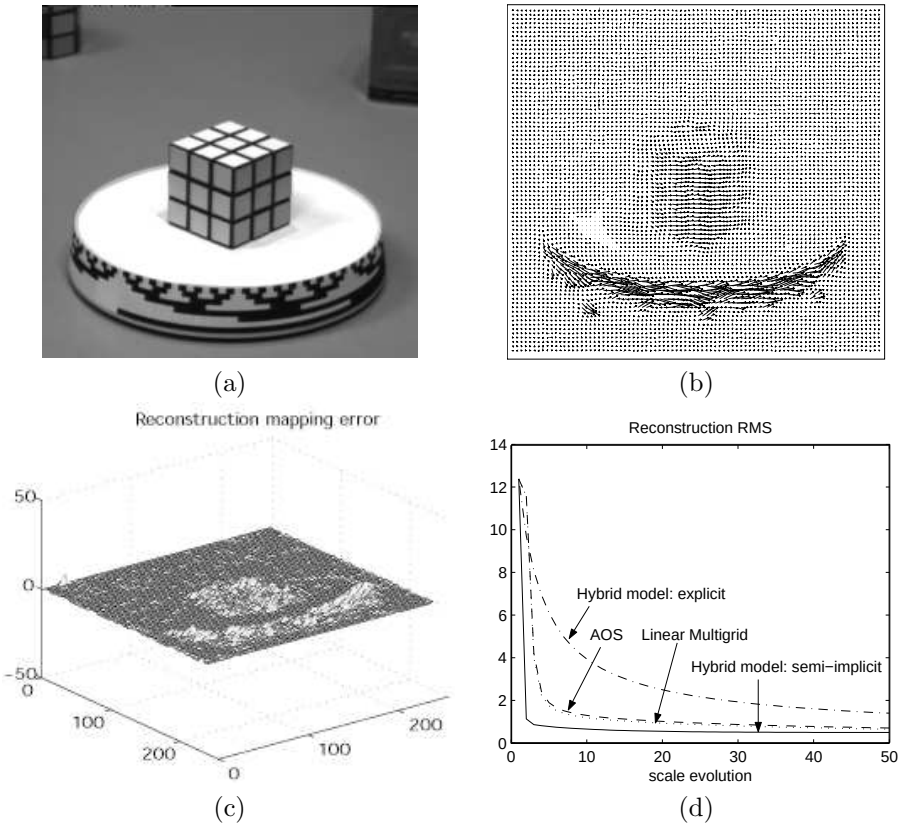

Figure 3. Performance on Rubic sequence, with $\alpha = 0.002, \tau = 4.0, \beta_{of} = 1.0, \beta_I = 0.01$, (a) image #10, (b) optical flow needle map, (c) reconstruction mapping error, (d) reconstruction RMS of different methods.

6. CONCLUSIONS

In this paper, we proposed a hybrid diffusion model for optical flow estimation, both image driven and flow driven information are used for the regularization terms of the linear anisotropic diffusion and nonlinear isotropic diffusion, respectively. Compared with the existing diffusion models for optical flow estimation, it can preserve the discontinuities in both magnitude and orientation. Furthermore, we developed the theoretical analysis to prove the existence, stability and uniqueness of the solution obtained using the proposed hybrid diffusion model. A semi-implicit scheme is proposed to implement the model with strong stability. From the experimental results, one can conclude that, the proposed hybrid diffusion model provides accurate estimation and fast convergence. The further analysis of influence in estimation results from numerical methods and the hybrid diffusion model itself respectively is under investigation.

Acknowledgement

This research has been partially conducted within the framework of the Inter-Universitary Attraction-Poles program number IAP 5/06 Advanced Mechatronic Systems, funded by the Belgian Federal Office for Scientific, Technical and Cultural Affairs. The authors would like to acknowledge the valuable comments and the two reference papers suggested by the referees.

REFERENCES

1. L. Alvarez, J.E. Monreal, M. Lefebure and J. Sánchez, A PDE model for computing the optical flow, In *Proceedings of CEDYA XVI*, Universidad de las Palmas de Gran, Canaria, September 1999, pp. 1349–1356.

2. L. Alvarez, J. Weickert and J. Sánchez, A scale-space approach to nonlocal optical flow calculations, In *Scale-Space Theories in Computer Vision*, (eds. M. Nielsen and P. Johansen), Springer-Verlag, Berlin, 1999, pp. 235–246.

3. L. Alvarez, J. Weickert and J. Sánchez, *Reliable Estimation of Dense Optical Flow Fields with Large Displacements*, Technical Report 2, Instituto Universitario de Ciencias y Tecnologias Ciberneticas,

Universidad de Las Palmas de Gran Canaria, Campus de Tafira, 35017 Las Palmas, Spain, November 1999.

4. T. Brox, A. Bruhn, N. Papenberg and J. Weickert, High accuracy optical flow estimation based on a theory for warping, In *Proceedings of the Eighth European Conference on Computer Vision*, Prague, Czech Republic, May 2004, pp. 25–36.

5. F. Catté, P.L. Lions, J.-M. Morel and T. Coll, Image selective smoothing and edge detection by nonlinear diffusion, *SIAM J. Numer. Anal.* (1992) **29**, 182–193.

6. R. Dautray and J.L. Lions (eds), *Mathematical Analysis and Numerical Methods for Science and Technology*, Vol.**5**, Evolution Problems I, Springer-Verlag, Berlin, 1988.

7. R. Deriche, P. Kornprobst and G. Aubert, Optical-flow estimation while preserving its discontinuities: A variational approach, In *Proceedings of the Second Asian Conference on Computer Vision*, Singapore, December 1995, pp. 290–295.

8. D. Geman and G. Reynolds, Constrained restoration and the recovery of discontinuities, *IEEE Transactions on Pattern Analysis and Machine Intelligence* (1992) **14**(3), 367–383.

9. W. Hinterberger, O. Scherzer, C. Schnörr and J. Weickert, *Analysis of Optical Flow Models in the Framework of Calculus of Variations*, Technical Report 8, Department of Mathematics and Computer Science, University of Mannheim, 68131 Mannheim, Germany, April 2001.

10. B. Horn and B. Schunck, Determining optical flow, *Artificial Intelligence* (1981) **17**, 185–203.

11. S.L. Keeling and R. Stollberger, Nonlinear anisotropic diffusion filtering for multiscale edge enhancement, *Inverse Problems* (2002) **18**(1), 175–190.

12. O.A. Ladyženskaja, V.A. Solonnikov and N.N. Ural'ceva, *Linear and Quai-linear Equations of Parabolic Type*, American Mathematical Society, 1968.

13. E. Mémin and P. Pérez, A multigrid approach to hierarchical motion estimation, In *Proceedings of Int. Conf. on Computer Vision (ICCV'98)*, Bombay, India, 1998, pp. 933–938.

14. H.H. Nagel and W. Enkelmann, An investigation of smoothness constraints for the estimation of displacement vector fields from image sequences, *IEEE Transactions on Pattern Analysis and Machine Intelligence* (1986) **8**(5), 565–593.

15. P. Perona and J. Malik, Scale space and edge detection using anisotropic diffusion, In *Proceedings of IEEE Comp. Soc. Workshop on Computer Vision*, Miami, USA, 1987, pp. 16–22.

16. M. Proesmans, E. Pauwels, and L. van Gool, Coupled geometry-driven diffusion equations for low-level vision, In *Geometry-driven Diffusion in Computer Vision*, (ed. B.M.H. Romeny), Kluwer Academic Publishers, Dordrecht, 1994, pp. 191–228.

17. D. Tschumperlé and R. Deriche, Constrainted and unconstrained PDE's for vector image restortaion. In *Proceedings of the Tenth Scandinavian Conf. Image Analysis*, (ed. I. Austvoll), Bergen, Norway, 2001, pp. 153–160.

18. J. Weickert, *Anisotropic Diffusion in Image Processing*, B. G. Teubner, Stuttgart, Germany, 1998.

19. J. Weickert, On discontinuity-preserving optic flow, In *Proceedings of Computer Vision and Mobile Robotics Workshop*, (eds. S. Orphanoudakis, P. Trahanias, J. Crowley and N. Katevas), Santorini, Greece, September 1998, pp. 115–122.

20. J. Weickert and C. Schnörr, *A Theoretical Framework for Convex Regularizers in PDE-based Computation of Image Motion*, Technical Report 13, Department of Mathematics and Computer Science, University of Mannheim, 68131 Mannheim, Germany, June 2000.

21. L.X. Yang, *Structure and Motion Analysis : Variational Methods and Related PDE Models*, PhD thesis, ETRO, Vrije Universiteit Brussel, Pleinlaan 2, B-1050 Brussel, Belgium, July 2004.